PHASE EQUILIBRIA OF METHANE CLATHRATE HYDRATE FROM GRAND CANONICAL MONTE CARLO SIMULATIONS

Matthew Lasich[a], Amir H. Mohammadi[a,b], Kim Bolton[c], Jadran Vrabec[d], Deresh Ramjugernath[a,*] [a] Thermodynamics Research Unit, University of KwaZulu-Natal, Durban, South Africa [b] Institut de Reserche en Génie Chimique et Pétrolier (IRGCP), Paris Cedex, France [c] School of Engineering, University of Borås, Borås, Sweden [d] Thermodynamik und Energietechnik, University of Paderborn, Paderborn, Germany

ABSTRACT

The determination of conditions at which clathrate hydrates are thermodynamically stable is important in applications such as offshore gas exploitation and energy storage. Adsorbed gas molecules occupy different cavity types within the hydrate lattice and this plays a significant role in the thermodynamic stability of clathrate hydrates. The occupancy of cavities in the hydrate lattice can be studied by undertaking Grand Canonical Monte Carlo simulations. Such simulations were performed in this study for methane clathrate hydrate with several force fields. Langmuir-type adsorption isotherms were fitted to the results of the simulations. The use of a single type of adsorption site was validated for methane clathrate hydrate. The adsorption isotherms which were fitted to the results of the simulations were used to compute the clathrate hydrate phase equilibria, which compared favourably with results from the literature.

1. INTRODUCTION

Clathrate hydrates are ice-like materials formed when inter-molecularly connected networks of water molecules enclathrate gas molecules, which are then trapped inside hydrogen-bonded crystal lattice structures. In nature, clathrate hydrates predominantly contain methane and can be found in permafrost or deep ocean deposits [1]. In industrial settings, clathrate hydrates form blockages in natural gas pipelines in offshore exploitation operations [2] and are a major area of concern [3]. Other areas of application of clathrate hydrates include their potential use as a storage medium for energy-carrier gases such as methane [4,5] and hydrogen [6,7], as a natural carbon sink on the Martian surface [8],and for use in industrial separation processes [9,10].

Three crystalline structures of clathrate hydrates are known: structure I (sI), structure II (sII), and structure H (sH) [1]. The sI clathrate hydrate contains two cavity types (small and large), with nominal radii of 0.395 and 0.433 nm, respectively [1]. The sII and sH clathrate hydrates have two and

three cavity types, respectively. The sH clathrate hydrate has greater relative differences in cavity radii than sI or sII [1]. This is illustrated in Table 1 [11], which summarises the crystalline structures of the different clathrate hydrate structures. The sI or sII clathrate hydrates are usually found in nature or industry because gas molecules can readily occupy both cavity types to a reasonable extent, thereby stabilising the clathrate hydrate. The larger difference in cavity radii of the sH clathrate hydrate results in a more pronounced size allowance for the gas molecules which can occupy the different cavity types. Therefore, only specific mixtures of small and large gas molecules can stabilize the sH clathrate hydrates, which results in this structure being less common. The use of computer simulations at the molecular level is well established as a complementary tool for research into adsorption of gases in clathrate hydrates [12–16]. An advantage of molecular simulations of clathrate hydrates over laboratory experiments is that the fractional occupancies of nanoscale cavities within the crystal lattice can be monitored directly. This is of interest as details of the physical mechanism or behaviour of clathrate hydrate formation or inhibition (depending upon the desired application) can yield improvements in industrial processes. For the case of natural gas exploitation, it is beneficial to inhibit the formation of clathrate hydrates within pipelines, thus reducing the cost to the consumer. In the case of energy storage, it is desirable to promote the formation and stability of clathrate hydrates to yield attractive materials for commercial use. Grand Canonical Monte Carlo (GCMC) simulations [17–19] in particular are useful to study gas adsorption in clathrate hydrates, as they provide information about the quantity of gas adsorbed and the spatial distribution of molecules within the crystal lattice. Moreover, purely hypothetical molecules can be investigated, providing insight into molecular behaviour of clathrate hydrates. This contribution studies adsorption of methane into sI clathrate hydrate by means of GCMC simulations, as well as phase equilibria calculated from these data. Comparisons are made with published results, and the use of GCMC simulations to study clathrate hydrate phase equilibria is illustrated.

Clathrate crystal structure	sI		sII		sH		
Crystal system	Primitive cubic		Face-centered cubic		Hexagonal		
Space group	*Pm3n*		*Fd3m*		*P6/mmm*		
Cavity type	Small	Large	Small	Large	Small	Medium	Large
Cavity description	5^{12}	$5^{12}6^2$	5^{12}	$5^{12}6^4$	5^{12}	$4^35^66^3$	$5^{12}6^8$
Cavities/unit cell	2	6	16	8	3	2	1
Cavity radius (nm)	0.395	0.433	0.391	0.473	0.391	0.406	0.571
H_2O/unit cell	46		136		34		
Unit cell formula	$2S{\cdot}6L{\cdot}46H_2O$		$16S{\cdot}8L{\cdot}136H_2O$		$3S{\cdot}2M{\cdot}1L{\cdot}34H_2O$		

Table 1. Summary of crystalline structures and properties of the three types of clathrate hydrate structures. In the unit cell formula S, M, and L denote small, medium, and large cavities, respectively [11].

A large fraction of adsorption sites may be occupied when using gas hydrates as an energy storage medium, since it can contain by volume, significant amounts of energy-carrier gases such as methane [4] or hydrogen [6,7,20]. Computational studies can provide occupancy data of adsorption sites directly, whereas experimental measurements are more complex or costly, and are often based on neutron diffraction [21–29]. There have been several computational studies of gas adsorption in clathrate hydrates. These include gases such as methane [13,16], hydrogen [14], carbon dioxide [16], xenon [12], and nitrogen [30]. Such studies have considered both flexible and rigid water lattices, and although the flexible lattice is inherently more rigorous, it was found that there was little qualitative difference between the results obtained via either approach. For the sake of rigour, flexible lattices were used in this study. Adsorption characteristics of clathrate hydrates do not directly reveal the conditions at which they are thermodynamically stable. However, it was suggested that there may be "equivalence between the coexistence line on the phase diagram and the con-tour of 90% total cage occupancy, corresponding to the stable methane hydrate" [13], and that this can provide qualitative assessment of thermodynamic stability of the hydrate through adsorption simulations. Moreover, phase equilibrium calculations of the stable hydrate region, performed using van der Waals–Platteeuw (vdWP) theory, make use of a cage occupancy term. Thus, the thermodynamically stable region can be estimated if the adsorption behaviour is known. Previous studies of adsorption in the sI methane clathrate hydrate do not fully agree on the adsorption mechanism. The vdWP theory states that there are two different types of adsorption sites (small and large), and that large sites are preferentially

occupied by gas species during adsorption. Computational studies by Sizov and Piotrovskaya [13] and Glavatskiy at al. [16] have suggested that there can be no distinction between small and large adsorption site types in methane clathrate hydrate (for the temperature ranges of T < 260 K, and 278 K ≤ T ≤ 328 K, respectively). These two studies also found that the Langmuir-type adsorption model did not fit the data. In contrast, Papadimitriou et al. [15] determined that adsorption of methane in sI clathrate hydrate can be described by adsorption in two distinct types of adsorption sites, and by Langmuir-type adsorption. Thus, this contribution examines which model can best describe the sI methane clathrate hydrate.

2. THEORY AND METHODS

2.1. CLATHRATE HYDRATE PHASE EQUILIBRIA

Phase equilibrium relations of clathrate hydrates were developed using statistical mechanics in vdWP theory [31], which describes the chemical potential of loaded clathrate hydrate in equilibrium with liquid water. There are several shortcomings of vdWP theory [32–42] due to assumptions made in its original formulation. These include the assumptions that there are no inter-molecular interactions between the gas species molecules and that there are no thermal vibrations of the water molecules in the crystal lattice. In spite of this, vdWP theory is frequently used to perform phase equilibrium calculations for clathrate hydrate systems since it yields data that is in reasonably good agreement with experimental results [43].

The internal partition function of the adsorbed methane molecules is assumed to be the same as that for the molecules in the gas phase [31]. Therefore, the phase equilibrium criterion is the equality between the chemical potential of liquid water (μ_w^l) and water in the hydrate phase (μ_w^H):

$$\mu_W^L = \mu_W^H \tag{1}$$

For convenience, the chemical potential of the hypothetical empty clathrate hydrate (μ_W^β) is used as a reference state:

$$\Delta\mu_W^L = \mu_W^\beta - \mu_W^L = \Delta\mu_W^H = \mu_W^\beta - \mu_W^H \quad (2)$$

The fractional occupancy of cavities in the clathrate hydrate by the gas species (θ) is used to calculate the difference between the chemical potential of water in loaded hydrate and the reference state ($\Delta\mu_W^H$):

$$\Delta\mu_W^H = -R \cdot T \cdot \sum_j [\, v_j \cdot \ln(1 - \sum_i \theta_{ij}) \,] \quad (3)$$

where index i refers to the gas species, j refers to cavity type (i.e., small, medium, large), v_j is the ratio of type j cavities to water molecules per unit cell in the hydrate lattice, and θ_{ij} is the fractional occupancy by gas species i of cavity type j. Langmuir-type adsorption [44] is often used to describe adsorption of the gas species into the cavities of the clathrate hydrate. GCMC simulations yield fractional occupancies of cavities directly. The use of this type of adsorption calculation with GCMC simulations is elaborated in Section 2.4.

The difference in chemical potential between water in the liquid phase and the reference state ($\Delta\mu_W^L$) may be expressed as the difference in chemical potential between two pure phases at a reference state ($\Delta\mu^0$) of T_R = 273.15 K and P_R = 0 MPa, considering the temperature and pressure dependence [45]:

$$(\Delta\mu_W^L) / (R \cdot T) = (\Delta\mu^0) / (R \cdot T_R) - \int_{TR}^{T} \Delta H_W / (R \cdot T^2) \cdot dT + \int_0^P \Delta V_W / (R \cdot T) \cdot dP \quad (4)$$

where ΔH_W and ΔV_W are the differences in enthalpy and molar volume, respectively, between liquid water and the reference state. The volume term (ΔV_W) is assumed constant over the temperature range of interest. The enthalpy term (ΔH_W) is expressed in terms of the difference in isobaric heat capacity between liquid water and the reference state (ΔC_{PW}):

$$\Delta H_W = \Delta H_W^0 + \int_{TR}^{T} \Delta C_{PW} \cdot dT \quad (5)$$

where ΔH_W^0 is the enthalpy difference at the reference conditions of T_R= 273.15 K and P_R= 0 MPa.

The original form [45] of Eq. (4) also includes a term correcting for the solubility of the gas species in the liquid phase. However, this term can be neglected as it is several orders of magnitude lower than the other contributions to the chemical potential [46,47]. Values used to calculate phase equilibria can be found in the literature [48].

The phase equilibria were calculated using the Nelder–Mead algorithm [49] with a tolerance of 10^{-12} to minimise the objective function, Eq. (2), by adjusting the system pressure or temperature as required. In this way, the dissociation pressure was calculated for each temperature, and vice versa. Only sI clathrate hydrates were considered, as methane clathrate hydrates naturally occur in this form [1].

2.2. CLATHRATE HYDRATE CRYSTAL STRUCTURE

The usual approach to calculate gas hydrates via vdWP theory[31] considers sI clathrate hydrate as having two separate adsorption sites onto which gas molecules are adsorbed according to a Langmuir-type mechanism. These sites are located at the centres of the small and large cavities within the unit cell.

The sI unit cell itself consists of 46 water molecules, with 2 small and 6 large cavities fully enclosed by hydrogen-bonded water molecules. These cavities can be considered (geometrically) as “cages”, with the small cage being formed by 12 pentagonal rings of water molecules, and the large cage being formed by 12 pentagonal rings and two hexagonal rings of water molecules [11]. Oxygen atoms form vertices of these polygonal rings, with hydrogen atoms lying along the edges. Nominal radii of the small and large cages are 0.395 nm and 0.433 nm, respectively [2]. It should be stated that although these cages are not spherical, a spherical approximation is often used in the literature, especially when determining the Langmuir constants to describe adsorption of gas molecules. Cages in sI clathrate hydrate are arranged in a primitive cubic manner, according to the Pm3n crystallographic space group, and the cell constant is 1.203 nm [1].

Clathrate hydrates are from a class of substances known as “clathrate compounds” which consist of networks of intermolecularly connected molecules of a “host” species “enclathrating”, or trapping, a

"guest" species. The sI hydrate is, in more general terms, a solution of the Kelvin problem which deals with the geometry of bubbles of equal volume which share minimum surface area when forming foam. The sI structure is the Weaire–Phelan structure [50] which is a superior solution to the previous optimal solution, the Kelvin conjecture [51]. In essence, the sI structure represents a system of cavities of roughly equal volume and thus it is reasonable to presume that in certain cases there can be guest particles which behave in a manner which suggests there is no distinction between the nominal types of cavities.

2.3. SIMULATION DETAILS

Methane adsorption characteristics of sI hydrates were studied by GCMC [17,18] computer simulations making use of the Metropolis scheme [19]. The General Utility Lattice Program [52]was used to perform these computations. The GCMC ensemble specifies the chemical potential (μ), volume (V), and temperature (T) of the system. Simulations were performed for 10^7 MC moves, and the first 25% were used to reach equilibrium, since the number of adsorbed gas molecules began to plateau after about 10^6 MC moves. The following types of MC moves were considered: translation/rotation, particle creation and destruction. The probability of selecting each type of move was 33.3%. The translation/rotation moves mimic the motion of molecules within the hydrate, and the creation and destruction moves (applied solely to the gas molecules) represent adsorption and desorption processes, respectively. Flexibility was allowed for the crystal lattice, for the sake of rigour. The maximum allowed translational displacement was 0.05 nm. The value of the chemical potential (see Figure 1)was estimated using the grand equilibrium ensemble [53] computer program "ms2" [54]. Chemical potential values obtained via the grand equilibrium ensemble simulations were then used in the GCMC simulations.

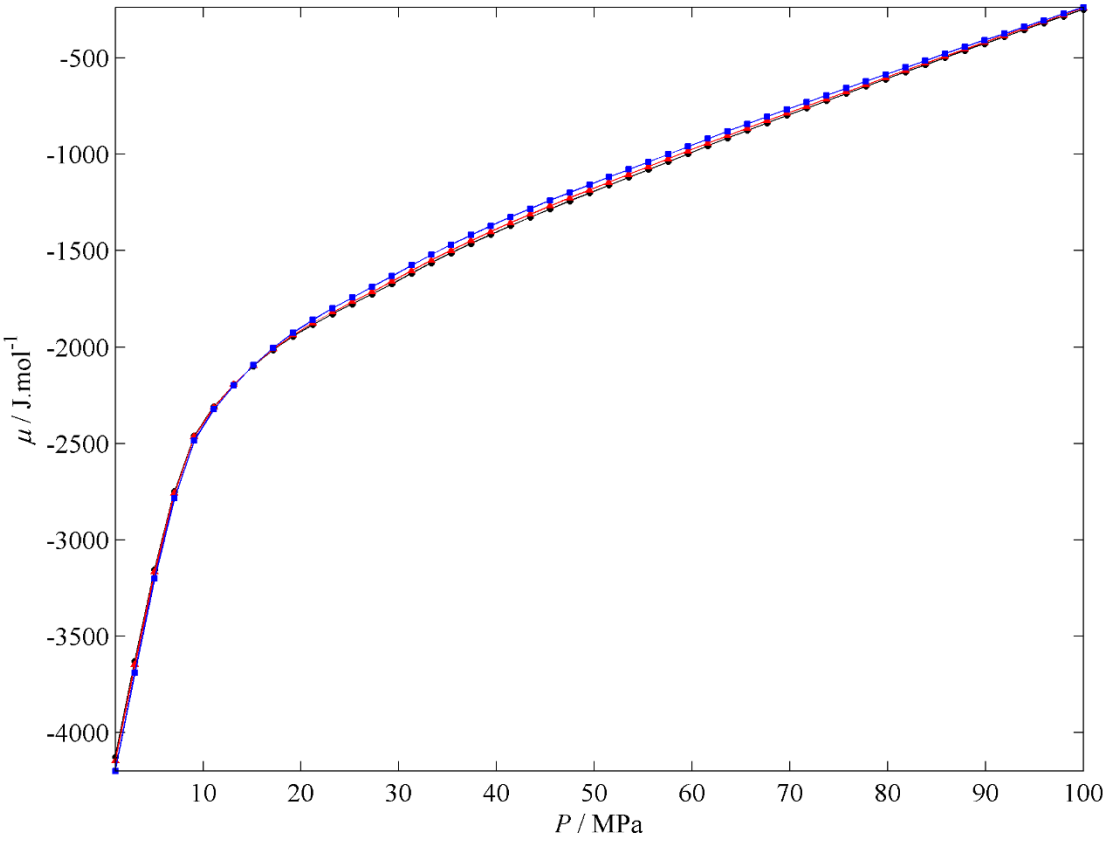

Figure 1. Chemical potential (μ) of methane versus pressure (P), estimated using the grand equilibrium ensemble [53,54]. (-O-) T = 273.2 K, (-Δ-) T = 280 K, and (-□-) T = 300 K.

For the grand equilibrium MC simulations, the system consisted of 500 methane particles. Relaxation for pre-equilibration consisted of 100 MC cycles, followed by 2×10^4 NVT cycles and 5×10^4 NPT steps for equilibration. 3×10^5 MC cycles were used for data production. Widom's method [55] was used to estimate the chemical potential, using 2000 test particles.

A single (i.e., 1 × 1 × 1) unit cell of sI methane clathrate hydrate was considered in the present GCMC simulations, since extensive studies of finite size effects have found negligible differences when using either a 1 × 1 × 1 or 2 × 2 × 2 unit cell [14,56]. A sI lattice structure from a previous computational study [57] was used, but the lattice constant was fine-tuned to 1.20 nm.

The same force fields were used for the grand equilibrium ensemble and GCMC simulations. The water molecules were described by the simple point charge (SPC) [58] or the TIP4P/ice [59] force fields, which allowed for comparison of the results obtained from these two models. Intermolecular

dispersion forces were modelled using the Lennard-Jones (LJ) potential [60]. Two different methane force fields were used: the transferable potentials for phase equilibrium (TraPPE) [61] force field, and another in which the LJ parameters were determined from the critical properties (i.e. critical temperature T_C= 190.6 K, and critical pressure P_C= 4.60 MPa) [62,63]. The force field parameters used in this study are presented in Table 2. Interaction between unlike LJ pairs was determined by the Lorentz [64] and Berthelot [65] combining rules. The cut-off radius was 1 nm for the LJ interactions and Ewald [66] summation was used for electrostatic long range interactions.

Force field	Non-bonded interactions (Lennard-Jones [58])	Charges	Bond angle
SPC water [58]	ε_O / k_B = 78.21 K	q_O = -0.82 e	$\alpha_{(H\text{-}O\text{-}H)}$ = 109.47 ^{o}
	σ_O = 0.3166 nm	q_H = +0.41 e	
TIP4P/Ice water [59]	ε_O / k_B = 106.1 K	q_O = -1.1794 e	$\alpha_{(H\text{-}O\text{-}H)}$ = 104.52 ^{o}
	σ_O = 0.31668 nm	q_H = +0.5897 e	
United atom LJ methane [62,63]	ε_{CH4} / k_B = 145.27 K		
	σ_{CH4} = 0.3821 nm		
TraPPE methane [61]	ε_{CH4} / k_B = 148.0 K		
	σ_{CH4} = 0.3730 nm		

Table 2 Force field parameters used in this study.

2.4. LANGMUIR-TYPE GAS ADSORPTION

The single-site Langmuir adsorption isotherm [44] is the simplest physically plausible description of the adsorption of gases onto solid surfaces [67]. Such adsorption isotherms are dependent upon temperature and the pressure of gas being adsorbed. This description is based upon three assumptions [67]: adsorption can only proceed up to a thickness of one layer of adsorbed gas molecules; all adsorption sites are equivalent; and the adsorption ability of any molecule at any site is independent of the occupation of neighbouring sites (i.e., there is no interaction between adsorbed gas molecules).

The Langmuir adsorption isotherm, or the number of adsorbed gas molecules per unit cell (N_i) for gas species *i*, can be expressed in terms of gas pressure (P_i), total number of adsorption sites per unit cell (N_T), and the Langmuir constant (C_i) [44]:

$$N_i = (C_i \cdot P_i \cdot N_T) / (1 + [C_i \cdot P_i]) \quad (6)$$

The quantity of interest in clathrate hydrate phase equilibria, however, is not the number of gas molecules adsorbed, but the fraction of cavities which are occupied, as required in Eq. (3). Therefore, it is necessary to express Eq. (6) such that the fraction of occupied adsorption sites is expressed as a function of P, C_i, and T. The fractional occupancy (θ) is defined as

$$\theta = N_i / N_T \quad (7)$$

It should also be noted that non-ideality of gas species can be accounted for in Eq. (6) by substitution of pressure by fugacity. For fitting the Langmuir constant and calculating phase equilibria, the fugacity was determined by the Peng–Robinson cubic equation of state [68]. This was to ensure consistency with the vdWP calculation, in which the Peng–Robinson equation of state is used in this study.

In order to determine whether Eq. (6) provides a valid description of the adsorption observed in experiments or from simulations, a linearised form is required [69]:

$$(P_i / N_i) = [(1 / N_T) \cdot P_i] + [1 / (C_i \cdot N_T)] \quad (8)$$

Thus, if a plot of P_i/N_i versus P_i is linear then a single-site Langmuir-type isotherm describes the observed adsorption. It should be noted that this type of verification calculation is biased towards higher pressures [67], and is therefore well-suited to clathrate hydrate systems, which are often under high pressure.

A useful relationship which can be used to describe temperature dependence of the Langmuir constant is in terms of parameters A_i and B_i fitted to various data sources [48]:

$$C_i = (A_i / T) \cdot \exp (B_i / T) \quad (9)$$

3. RESULTS AND DISCUSSION

3.1. SINGLE SITE ADSORPTION

Figure 2 shows a snapshot for the SPC water + united-atom LJ methane clathrate hydrate system at T = 273.2 K and P = 3 MPa, after 9310748 MC moves. Results of the GCMC simulations, expressed in the form of Eq. (8), are presented in Figures 3 through 5. It is apparent that the results for all force fields exhibit a linear trend when considering both pressure and fugacity. This suggests that there is no significant difference whether methane is treated as an ideal or non-ideal gas under the conditions in this study. The correlation coefficients for linear trends fitted to the data for all isotherms were greater than 0.997, and all trend lines lie within the statistical uncertainties of the GCMC simulations.

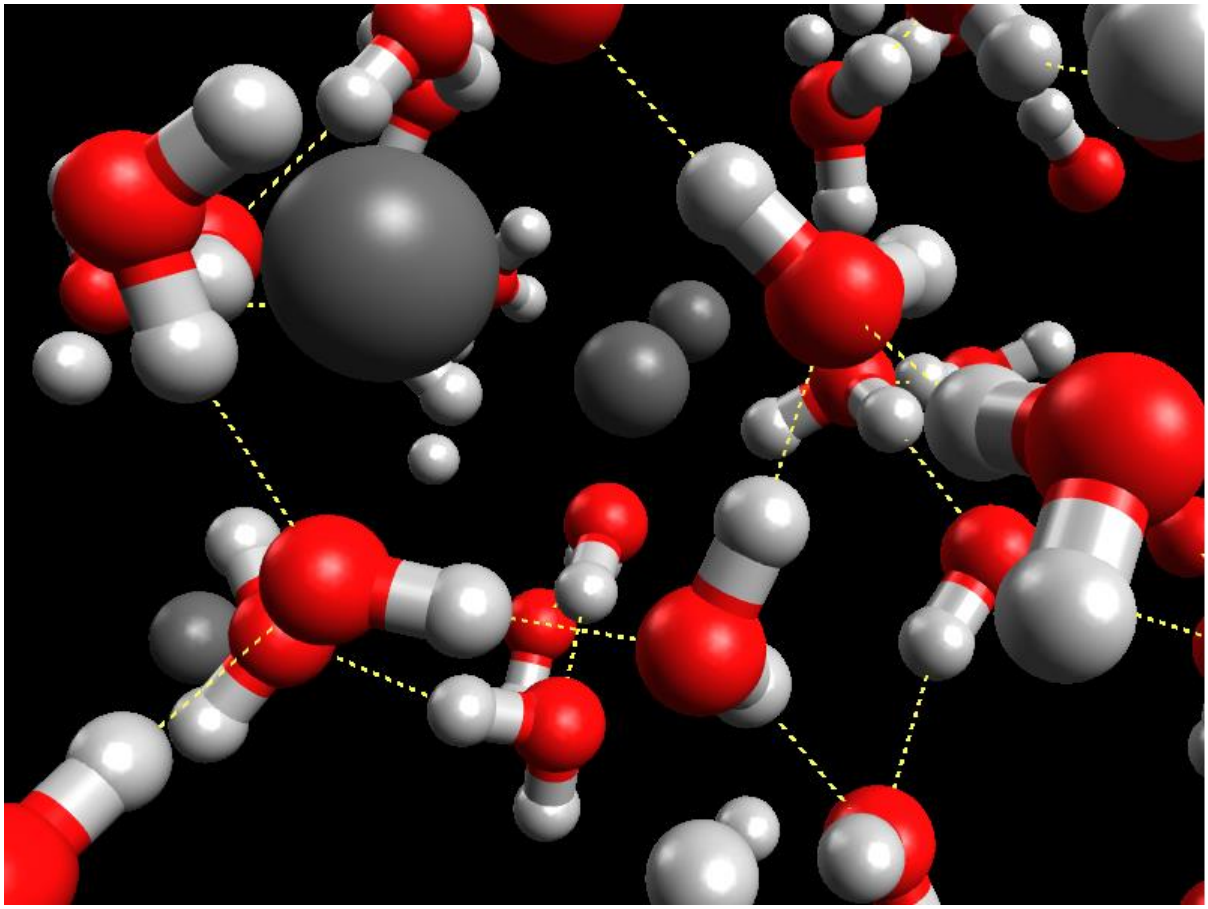

Figure 2. Snapshot of the SPC water + united-atom LJ methane clathrate hydrate system at T = 273.2 K and P = 3 MPa, after 9310748 MC moves. The dashed lines represent hydrogen bonds between the 3-site water molecules. Methane molecules are represented by lone, unconnected, dark grey particles inside the clathrate lattice.

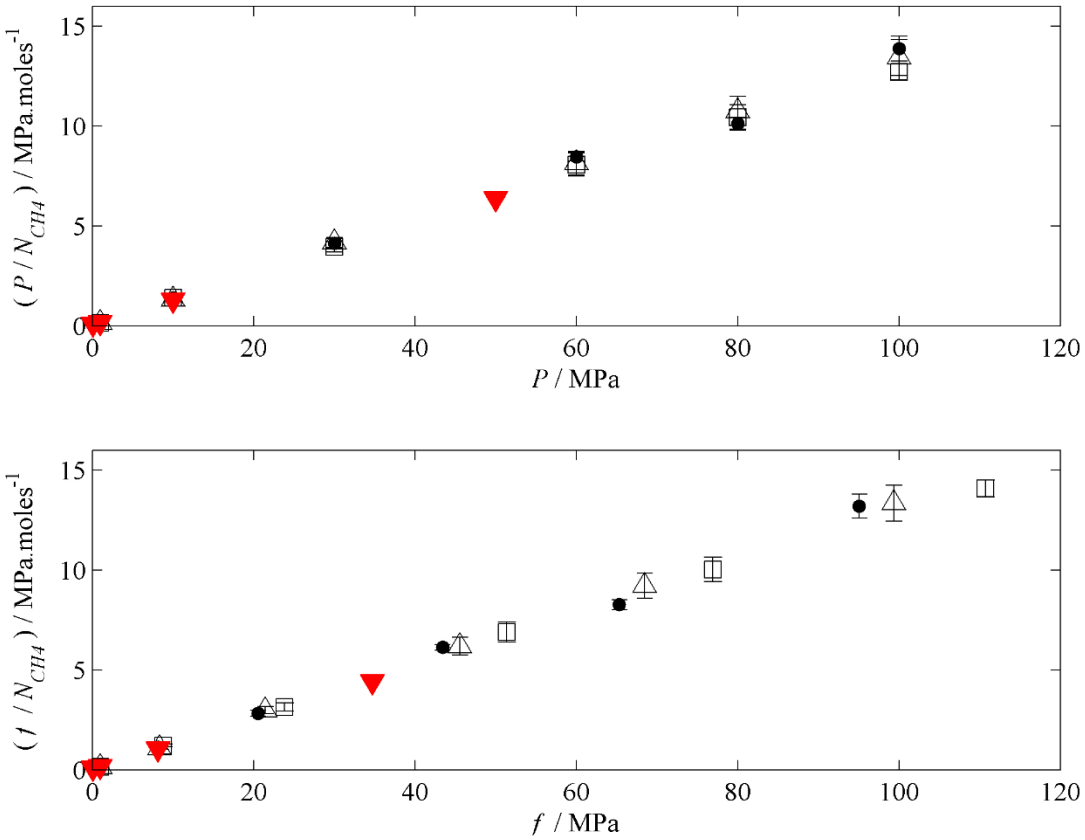

Figure 3. Linearised Langmuir-type adsorption isotherms for sI SPC water + united-atom LJ methane clathrate hydrate; see Eq. (8). The upper plot employs pressure (*P*) (i.e., assumption of ideal gas behaviour for methane), and the lower plot uses fugacity (*f*) in Eq. (8). NCH4 is the number of moles of methane adsorbed per mole of the crystal unit cell. System at: (●) *T* = 273.2 K, (Δ) *T* = 280 K, and (□) *T* = 300 K. Adsorption isotherms obtained by Papadimitriou and co-workers [15] at *T* = 273 K: (▼).

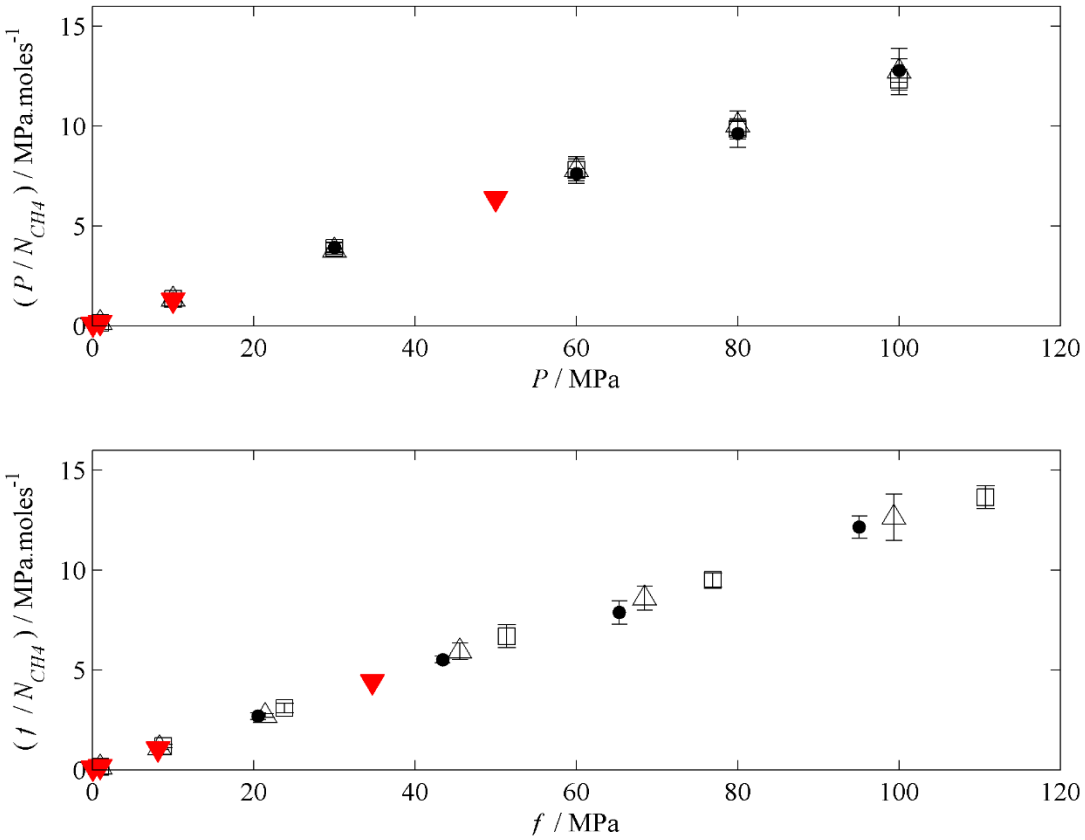

Figure 4. Linearised Langmuir-type adsorption isotherms for sI SPC water + TraPPE methane clathrate hydrate; see Eq. (8). The upper plot employs pressure (*P*) (i.e., assumption of ideal gas behaviour for methane), and the lower plot uses fugacity (*f*) in Eq. (8). NCH4 is the number of moles of methane adsorbed per mole of the crystal unit cell. System at: (●) *T* = 273.2 K, (Δ) *T* = 280 K, and (□) *T* = 300 K. Adsorption isotherms obtained by Papadimitriou and co-workers [15] at *T* = 273 K: (▼).

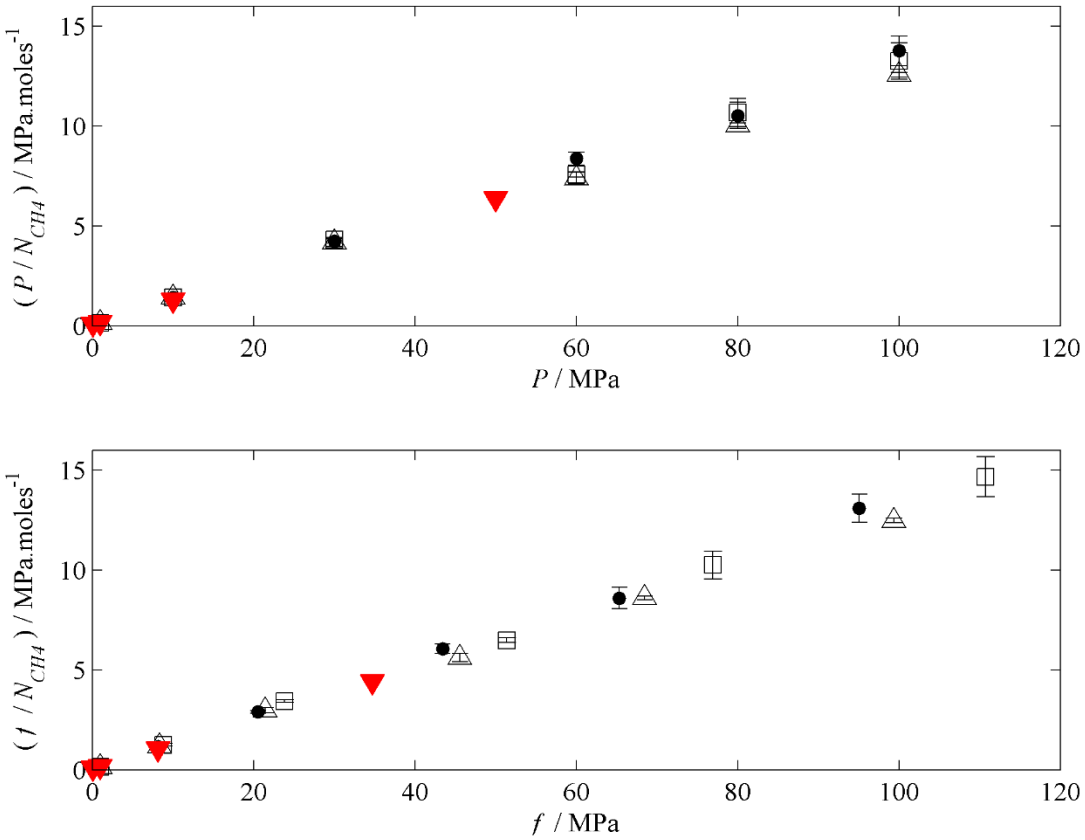

Figure 5. Linearised Langmuir-type adsorption isotherms for sI TIP4P/ice water + united-atom LJ methane clathrate hydrate; see Eq. (8). The upper plot employs pressure (*P*) (i.e., assumption of ideal gas behaviour for methane), and the lower plot uses fugacity (*f*) in Eq. (8). NCH4 is the number of moles of methane adsorbed per mole of the crystal unit cell. System at: (●) *T* = 273.2 K, (Δ) *T* = 280 K, and (□) *T* = 300 K. Adsorption isotherms obtained by Papadimitriou and co-workers [15] at *T* = 273 K: (▼).

Examination of the occupancy at the molecular level (using spatial coordinate data) showed gas molecules at all adsorption sites. Statistical uncertainties of occupancy data for the "small" cavities were substantial, and made it difficult to distinguish between adsorption at the two types of sites. For this reason, Eq. (8) was used to further examine the plausibility of using a single type of adsorption site. It should also be noted that the reciprocals of the slopes of the linear trends described by Eq. (8) yielded a range of$6.3 < N_T < 7.1$, which further corroborates the fact that gas molecules are adsorbed at all site (as mentioned above there are 8 sites in the unit cell used in the simulations).

The linearity present in Figures 3 through 5 suggests that adsorption of methane into sI clathrate hydrates can be described in terms of a single type of Langmuir site. This is evidenced by the linear trends in Figures 3 through 5. The correlation coefficients (R^2) for each of the linear trends (averaged

for each force field combination) are shown in Table 3, and it is clear that all are highly linear (R^2= 0.999 in all cases, with a minimum of R^2= 0.997). The validity of a single Langmuir-type adsorption site suggests that, from the perspective of methane molecules being adsorbed, there is no clear distinction between cavity types in the hydrate lattice. This can be due to the size of methane molecules relative to the cavities; $\sigma_{CH4} \approx 0.38$ nm (see Table 2), while the small and large cavity radii are 0.395 and0.433 nm, respectively (see Table 1). This significant size differential between methane molecules and cavities in the hydrate lattice resulted in the probability of acceptance during the adsorption process being about the same for both small and large cavities (within the statistical uncertainties).

Force fields	A_i / K·MPa^{-1}	B_i / K	AAD / %	R^2
SPC water + united atom LJ methane	19.129	$1.3121 \cdot 10^3$	6.3	0.999
SPC water + TraPPE methane	18.276	$1.5073 \cdot 10^3$	2.7	0.999
TIP4P/Ice water + united atom LJ methane	10.392	$1.5183 \cdot 10^3$	7.3	0.999

Table 3. Fitted parameters for Langmuir-type adsorption isotherms [44] obtained from GCMC simulations; see Eq. (9). AAD is the absolute average deviation of fitted adsorption isotherms to GCMC simulation results from this study, and R^2 is the average correlation coefficient of linear fits to the adsorption isotherms.

It should be noted, however, that this lack of differentiation in the adsorption of methane into the usual two cavity types can be considered as an approximation. Strictly speaking, there can be a differentiation in the adsorption of methane molecules into the cavity types. However, the statistical uncertainties of the results of the GCMC simulations of around 5–9%, and in the results of laboratory experiments of around 2–15% [70] should also be considered in this analysis. Therefore, results shown in Figures 3 through 5 suggest that the differentiation between cavity types in sI methane clathrate hydrates can be neglected, as this approximation is within the limits of the expected uncertainties in fractional occupancies of cavities within the hydrate lattice.

A consequence of considering only a single cavity type for certain clathrate hydrates is that in fitting Eq. (9) to experimental data, only two parameters are required, instead of the usual two parameters per cavity type. Thus, fewer data points are needed for regression. Future GCMC simulations will focus on the size range of the gas molecules in which this simplification is valid.

3.2. ADSORPTION ISOTHERMS

Parameters required to estimate the Langmuir constants by Eq. (9) are presented in Table 3, with average absolute deviation (AAD) of fitted equations with respect to results of GCMC simulations. Fit-ting was undertaken by comparing calculated occupancies ($\theta_{Calc.}$) and occupancies from GCMC simulations ($\theta_{Sim.}$, see Eq. (8)), using the sum of squared errors (SSE) adjusted for uncertainties in simulations (u_i) as follows:

$$SSE = \sum_i [(\theta_{Calc.} - \theta_{Sim.})_i^2 / u_i] \quad (10)$$

This adjustment can limit the fitting procedure from favouring data which are associated with large uncertainties. The occupancies are considered as the fraction of the total number of adsorption sites(i.e., 8 in the sI clathrate hydrate) which are occupied by methane molecules.

It should also be mentioned that in order to describe retrograde phase behaviour of methane clathrate hydrate, an explicit pressure dependence of the Langmuir constants could be considered [71].However, pressure dependence would only influence the phase equilibria at very high pressures. The simulations considered in this study reached a maximum pressure of 100 MPa, and so this may not be applicable for the results shown. This will be investigated in future studies.

There is some disparity between the AAD values presented in Table 3 and the linearity (described by the R^2 values) of the Langmuir isotherm trend lines shown in Figures 3 through 5. The significantly larger absolute average deviations for the fit-ted adsorption isotherms using Eq. (9) arise as an artefact of the temperature-dependence fitting. This is not a shortcoming of the Langmuir adsorption isotherm itself, but of the form of the temperature dependence which is commonly used.

3.2. PHASE EQUILIBRIA

Phase equilibria of methane clathrate hydrates are shown in Figure 6, expressed in terms of dissociation pressure versus temperature. The calculated phase equilibria from this study are compared to calculations using Langmuir-type isotherms reported in the literature [15,48] as well as

to experimental results [72,73]. It can be seen that the present simulations agree with calculations from the literature [15], within estimated statistical uncertainties. Uncertainties were derived from the maximum fractional deviations of Langmuir-type adsorption isotherms fitted to results of GCMC simulations. It should be noted that this study uses only two adjustable parameters (A_i and B_i), as opposed to the four parameters (A_i and B_i for both the small and large cavities) from the literature [15]. Considering two types of cavities in the hydrate lattice does not result in a significant improvement of the calculated phase equilibria as compared to the assumption of a single effective cavity type.

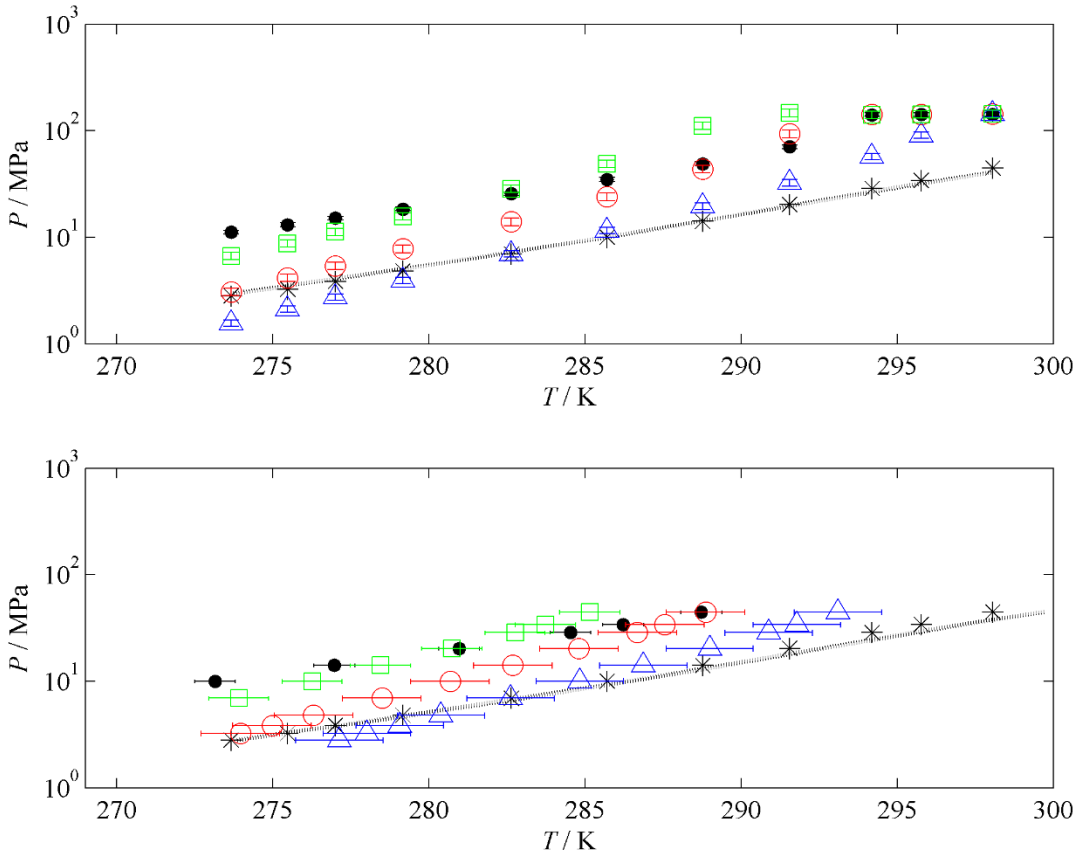

Figure 6. Dissociation pressure (*P*) versus temperature (*T*) for sI methane clathrate hydrate. The upper plot was determined by varying *P*, and the lower plot by varying *T* in Eq. (2). Calculated phase equilibria based on Langmuir-type adsorption isotherms fitted to GCMC data: (●) previous study [15], (Δ) SPC water + TraPPE methane, and (O) SPC water + united atom LJ methane, (□) TIP4P/ice water + united atom LJ methane, (∗) experimental measurements [72,73], and (· · ·) calculated phase equilibria [48].

Another point of interest is the apparent convergence between calculated phase equilibria and experimental measurements at high pressures. It was previously [12] found that the free energy of clathrate hydrates calculated from GCMC simulations converges with the directly calculated free energy at high pressures. The convergence seen for the calculated phase equilibria in this study also suggests that agreement between GCMC simulations and the real clathrate hydrate systems improves at high pressures.

Figure 7 compares the results of this study with a previous study which used molecular dynamics (MD) simulations to determine the direct coexistence [74] for a united atom LJ methane using parameters from two sources [75,76] with several water force fields: TIP4P [77], TIP4P/2005 [78], and TIP4P/ice [59]. The influence of adjusting a binary correction factor (k_{ij}) for the Berthelot rule applied for the cross-interaction in the dispersion parameter (ε) between intermolecular LJ sites *i* and *j* is also shown. This correction factor is applied as:

$$\varepsilon_{ij} = k_{ij} \cdot (\varepsilon_i \cdot \varepsilon_j)^{0.5} \tag{11}$$

The adjustment to k_{ij} shown in Eq. (11) was performed indirectly, by fitting the excess chemical potential of dilute methane in liquid water [79].

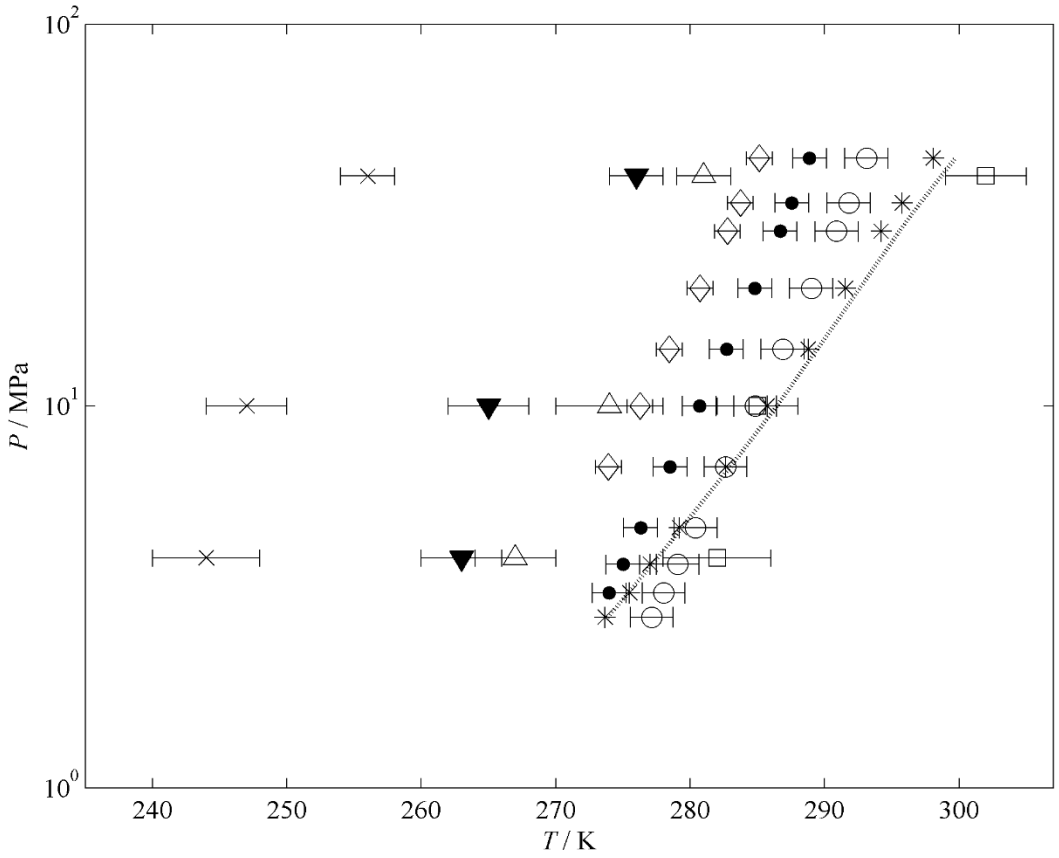

Figure 7. Dissociation pressure (*P*) versus temperature (*T*) for sI methane clathrate hydrate. Calculated phase equilibria based on Langmuir-type adsorption isotherms fitted to GCMC data: (●) SPC water + TraPPE methane, (o) SPC water + united atom LJ methane, (◊) TIP4P/ice water + united atom LJ methane. Direct coexistence simulations [74] using a different united atom LJ methane [75,76]: (×) TIP4P water, (▼)TIP4P/2005, (Δ) TIP4P/2005 with k_{ij} = 1.07 (see Eq. (11)), (□) TIP4P/ice. (∗) experimental measurements [72,73], (· · ·) calculated phase equilibria [48].

It is apparent that the phase equilibria calculated in this study from GCMC simulations compare favourably with results of direct coexistence MD simulations. A comparison of the deviations in terms of temperature is presented in Table 4. In particular, only direct coexistence MD simulations performed using TIP4P/ice water performed as well as the GCMC simulations in predicting experimental phase equilibria. Generally, the phase equilibria obtained using direct coexistence MD and GCMC simulations are comparable when using various combinations of force fields. Therefore, GCMC simulations provide a valid method to determine Langmuir-type adsorption isotherms which can then be used to calculate clathrate hydrate phase equilibria.

Figure 7 also shows that the force field can be fine-tuned to yield results that are in better agreement with experiment. These changes can possibly be applied to cross-interactions between methane and

water LJ sites via Eq. (11). This can be done using experimental dissociation pressures, by means of Langmuir-type adsorption isotherm fitting to the results of GCMC simulations. As stated previously, the determination of binary correction factors has been undertaken more indirectly in the past, such as via the excess chemical potential of dilute methane in liquid water [79]. For the purposes of flow assurance in offshore gas exploitation, where phase equilibria are of direct interest, it could be more useful to make a direct comparison with available experimental measurements.

It was also found that phase equilibria calculated in this study using parameters derived from GCMC simulations employing the SPC force field yielded better predictions of the experimental data than with TIP4P/ice water. The TIP4P/ice system from this study did not fit as well as a previous study using direct coexistence MD simulation. [74], which could be due to the other parameters in the phase equilibrium calculation (see Eqs. (1)–(5)).

Force fields	Method	Source	AAD / K	AAD / %
SPC water + united atom LJ methane	GCMC adsorption	This study	5.3	1.8
SPC water + TraPPE methane	GCMC adsorption	This study	2.4	0.8
TIP4P/Ice water + united atom LJ methane	GCMC adsorption	This study	10.8	3.7
SPC/E water + OPLS-UA methane	GCMC adsorption	[15]	10.6	3.6
TIP4P water + united atom LJ methane	Direct coexistence MD	[74]	38.0	13.2
TIP4P/2005 water + united atom LJ methane	Direct coexistence MD	[74]	19.0	6.6
TIP4P/2005 water (k_{ij} = 1.07) + united atom LJ methane	Direct coexistence MD	[74]	13.0	4.5
TIP4P/Ice water + united atom LJ methane	Direct coexistence MD	[74]	3.3	1.2

Table 4. Comparison of different data sets in terms of the deviation from experimental dissociation temperature of methane clathrate hydrate. AAD is the absolute average deviation of calculated (this study and [15]) and simulated [74] phase equilibria to experimental data [72,73].

3.4. HEAT OF DISSOCIATION

Once the phase equilibria are known, the heat of dissociation ($\Delta H_{Diss.}$) can be calculated from the Clausius–Clapeyron equation [80]:

$$\mathrm{d}\ln P / \mathrm{d}\left(1 / T \right) = - \Delta H_{Diss.} / \left(Z \cdot R \right) \qquad (12)$$

where Z is the compressibility factor of methane. This can be readily determined by forming a linear relationship between $\ln P$ and $1/T$. The results of this are shown in Table 5. For the purposes of this comparison, the compressibility factor of methane was fixed at unity. This would result in the lack of a temperature dependence for the heat of dissociation, although this is not expected to make a significant difference in the calculated value. It is apparent that the GCMC simulations overestimate the heats of dissociation, and it is therefore not always possible to obtain a close fit to the experimental phase equilibrium data (see Table 4) while simultaneously predicting a favourable heat of dissociation. However, it can be noted that molecular simulations generally appear to have poor predictive power when estimating the heat of dissociation of methane clathrate hydrate.

As with the calculated phase equilibria, the results from this study compare well with published values obtained via molecular simulation. The value obtained in this study for heat of dissociation for the system containing TIP4P/ice water compares favourably with a previous study [74] which also employed TIP4P/ice water, although in direct coexistence molecular dynamics simulations.

Force fields	Method	Source	$\Delta H_{Diss.}$ / kJ.mol^{-1}	AD / %
SPC water + united atom LJ methane	GCMC adsorption	This study	113.6	45.7
SPC water + TraPPE methane	GCMC adsorption	This study	115.5	48.1
TIP4P/Ice water + united atom LJ methane	GCMC adsorption	This study	102.5	31.1
SPC/E water + OPLS-UA methane	GCMC adsorption	[15]	62.5	19.9
TIP4P water + united atom LJ methane	Direct coexistence MD	[74]	95.5	22.5
TIP4P/2005 water + united atom LJ methane	Direct coexistence MD	[74]	96.9	24.3
TIP4P/2005 water (k_{ij} = 1.07) + united atom LJ methane	Direct coexistence MD	[74]	102.4	31.3
TIP4P/Ice water + united atom LJ methane	Direct coexistence MD	[74]	73.9	5.3
Experimental		[72,73]	78.0	
Calculated	vdWP calculation	[48]	73.6	5.6

Table 5. Heat of dissociation ($\Delta H_{Diss.}$) of methane clathrate hydrate calculated from phase equilibrium data. AD is the absolute deviation from the value calculated from experimental data. The methane gas was assumed to be ideal (i.e., $Z = 1$ in Eq. (12)) for this comparison.

4. CONCLUSIONS

GCMC simulations were used in conjunction with a linearized Langmuir gas adsorption model to show that considering only a single gas adsorption site is valid for sI methane clathrate hydrate. A temperature dependent Langmuir-type adsorption isotherm was then fitted to the present GCMC simulation results.

Phase equilibrium calculations were performed for methane clathrate hydrate using fitted Langmuir-type adsorption isotherms. The calculated phase equilibria compared favourably with previous simulations [15,74] and experiments [72,73]. The calculated phase equilibria were then used to estimate the heat of dissociation of methane clathrate hydrate. The value obtained for the system

containing TIP4P/ice water in this study compares favourably with a previous study [74] employing TIP4P/ice water in direct coexistence molecular dynamics simulations.

The results presented in this study demonstrate that GCMC simulations can be used to determine clathrate hydrate phase equilibria, and also show that using a single Langmuir-type adsorption site provides a valid description for methane clathrate hydrate.

ACKNOWLEDGEMENTS

This work is based on research supported by the South African Research Chairs Initiative of the Department of Science and Technology and National Research Foundation. The authors would like to thank the NRF Focus Area Programme and the NRF Thuthuka Programme, as well as the Swedish International Development Cooperation Agency. Thanks are due to Stiftelsen FöreningsSparbanken, who financed the computing facilities at the University of Borås. The authors would also like to thank the CSIR Centre for High Performance Computing in Cape Town for the use of their computing resources.

REFERENCES

[1] E.D. Sloan, C.A. Koh, Clathrate Hydrates of Natural Gases, CRC Press, Boca Raton,2008.
[2] E.G. Hammerschmidt, Ind. Eng. Chem. 26 (1934) 851–855.
[3] Welling and Associates, 1999 Survey, cited by N. Macintosh, Flow AssuranceStill Leading Concern among Producers, Offshore, October, 2000.
[4] S. Thomas, R.A. Dawe, Energy 28 (2003) 1461–1477.
[5] A.A. Khokhar, J.S. Gudmundsson, E.D. Sloan, Fluid Phase Equilib. 150 (1998)383–392.
[6] W.L. Mao, H.K. Mao, A.F. Goncharov, V.V. Struzhkin, Q. Guo, J. Hu, J. Shu, R.J.Hemley, M. Somayazulu, Y. Zhao, Science 297 (2002) 2247–2249.
[7] L.J. Florusse, C.J. Peters, J. Schoonman, K.C. Hester, C.A. Koh, S.F. Dec, K.N. Marsh,E.D. Sloan, Science 306 (2004) 469–471.
[8] S.L. Miller, W.D. Smythe, Science 170 (1970) 531–533.
[9] H. Kubota, K. Shimizu, Y. Tanaka, T. Makita, J. Chem. Eng. Jpn. 17 (1984) 423–429.
[10] S.P. Kang, H. Lee, Environ. Sci. Technol. 34 (2000) 4397–4400.

[11] N.I. Papadimitriou, I.N. Tsimpanogiannis, A.K. Stubos, Colloids Surf. A: Physic-ochem. Eng. Aspects 357 (2010) 67–73.

[12] H. Tanaka, Fluid Phase Equilib. 144 (1998) 361–368.

[13] V.V. Sizov, E.M. Piotrovskaya, J. Phys. Chem. B 111 (2007) 2886–2890.

[14] N.I. Papadimitriou, I.N. Tsimpanogiannis, A.Th. Papaioannou, A.K. Stubos, J.Phys. Chem. C 112 (2008) 10294–10302.

[15] N.I. Papadimitriou, I.N. Tsimpanogiannis, A.K. Stubos, Proceedings of the 7thInternational Conference on Clathrate Hydrates, Edinburgh, United Kingdom, 2011.

[16] K.S. Glavatskiy, T.J.H. Vlugt, S. Kjelstrup, J. Phys. Chem. B 116 (2012) 3745–3753.

[17] M.P. Allen, D.J. Tildesley, Computer Simulations of Liquids, Clarendon Press,Oxford, 1987.

[18] D. Frenkel, B. Smit, Understanding Molecular Simulation, Academic Press, SanDiego, 2002.

[19] N. Metropolis, A.W. Rosenbluth, M.N. Rosenbluth, A.H. Teller, E. Teller, J. Chem.Phys. 21 (1953) 1087–1092.

[20] W.L. Mao, H.-K. Mao, Proc. Natl. Acad. Sci. U. S. A. 101 (2004) 708–710.

[21] W.F. Kuhs, B. Chazallon, P.G. Radaelli, F. Pauer, J. Inclusion Phenom. Mol. Recog-nit. Chem. 29 (1997) 65–77.

[22] B. Chazallon, W.F. Kuhs, J. Chem. Phys. 117 (2002) 308–320.

[23] S. Sasaki, S. Hori, T. Kume, H. Shimizu, J. Chem. Phys. 118 (2003) 7892–7897.

[24] H. Itoh, J.S. Tse, K. Kawamura, J. Chem. Phys. 115 (2001) 9414–9420.

[25] H. Hirai, Y. Uchihara, Y. Nishimura, T. Kawamura, Y. Yamamoto, T. Yagi, J. Phys.Chem. B 106 (2002) 11089–11092.

[26] A.G. Ogienko, A.V. Kurnosov, A.Y. Manakov, E.G. Larionov, A.I. Ancharov, M.A.Sheromov, A.N. Nesterov, J. Phys. Chem. B 110 (2006) 2840–2846.

[27] A.Yu. Manakov, A.G. Dyadin, A.V. Ogienko, E. Kurnosov, E.G.Ya. Aladko, F.V. Lar-ionov, V.I. Zhurko, I.F. Voronin, S.V. Berger, A. Goryainov, A.I.Yu. Lihacheva, A.I.Ancharov, J. Phys. Chem. B 113 (2009) 7257–7262.

[28] H. Hirai, K. Komatsu, M. Honda, T. Kawamura, Y. Yamamoto, T. Yagi, J. Chem.Phys. 133 (2010) 124511.

[29] K.A. Lokshin, Y. Zhao, D. He, W.L. Mao, H.-K. Mao, R.J. Hemley, M.V. Lobanov, M. Greenblatt, Phys. Rev. Lett. 93 (2004) 125503.

[30] I.N. Tsimpanogiannis, N.I. Papadimitriou, A.K. Stubos, Mol. Phys. 110 (2012)1213–1221.

[31] J.H. van der Waals, J.C. Platteeuw, Adv. Chem. Phys. 2 (1959) 1–57.

[32] V.T. John, G.D. Holder, J. Phys. Chem. 85 (1981) 1811–1814.

[33] V.T. John, G.D. Holder, J. Phys. Chem. 86 (1982) 455–459.

[34] V.T. John, G.D. Holder, J. Phys. Chem. 89 (1985) 3279–3285.

[35] V.T. John, K.D. Papadopoulos, G.D. Holder, AIChE J. 31 (1985) 252–259.

[36] P.M. Rodger, J. Phys. Chem. 94 (1990) 6080–6089.

[37] K.A. Sparks, J.W. Tester, J. Phys. Chem. 96 (1992) 11022–11029.
[38] B. Kvamme, A. Lund, T. Hertzberg, Fluid Phase Equilib. 90 (1993) 15–44.
[39] K.A. Sparks, J.W. Tester, Z. Cao, B.L. Trout, J. Phys. Chem. B 103 (1999)6300–6308.
[40] Z. Cao, J.W. Tester, K.A. Sparks, B.L. Trout, J. Phys. Chem. B 105 (2001)10950–10960.
[41] B.J. Anderson, J.W. Tester, B.L. Trout, J. Phys. Chem. B 108 (2004)18705–18715.
[42] B.J. Anderson, M.Z. Bazant, J.W. Tester, B.L. Trout, J. Phys. Chem. B 109 (2005)8153–8163.
[43] P. Englezos, Ind. Eng. Chem. Res. 32 (1993) 1251–1274.
[44] I. Langmuir, J. Am. Chem. Soc. 38 (1916) 2221–2295.
[45] G.D. Holder, S. Zetts, N. Pradhan, Rev. Chem. Eng. 5 (1988) 1–70.
[46] L. Jensen, Experimental Investigation and Molecular Simulation of Gas Hydrates(Ph.D. Thesis), Technical University of Denmark, 2010.
[47] L. Jensen, K. Thomsen, N. von Solms, S. Wierzchowski, M.R. Walsh, C.A. Koh, E.D. Sloan, D.T. Wu, A.K. Sum, J. Phys. Chem. B 114 (2010) 5775–5782.
[48] W.R. Parrish, J.M. Prausnitz, Ind. Eng. Chem. Process Des. Dev. 11 (1972) 26–34.
[49] J.A. Nelder, R. Mead, Comput. J. 7 (1965) 308–313.
[50] D. Weaire, R. Phelan, Philos. Mag. Lett. 69 (1994) 107–110.
[51] W. Thompson, Lord Kelvin, Philos. Mag. 24 (1887) 503–514.
[52] J.D. Gale, A.L. Rohl, Mol. Sim. 29 (2003) 291–341.
[53] J. Vrabec, H. Hasse, Mol. Phys. 100 (2002) 3375–3383.
[54] S. Deublein, B. Eckl, J. Stoll, S.V. Lishchuk, G. Guevara-Carrion, C.W. Glass, T. Merker, M. Bernreuther, H. Hasse, J. Vrabec, Comput. Phys. Commun. 182 (2011)2350–2367.
[55] B. Widom, J. Chem. Phys. 39 (1963) 2808–2812.
[56] N.I. Papadimitriou, I.N. Tsimpanogiannis, A.Th. Papaioannou, A.K. Stubos, Mol.Sim. 34 (2008) 1311–1320.
[57] A. Lenz, L. Ojamäe, J. Phys. Chem. A 115 (2011) 6169–6176.
[58] H.J.C. Berendsen, P.J.M. Postma, W.F. van Gunsteren, J. Hermans, in: B. Pullman (Ed.), Intermolecular Forces, Reidel, Dordrecht, 1981, pp. 331–342.
[59] J.L.F. Abascal, E. Sanz, R.G. Fernandez, C. Vega, J. Chem. Phys. 122 (2005) 234511.
[60] J.E. Lennard-Jones, Proc. Phys. Soc. 43 (1931) 461–482.
[61] M.G. Martin, J.I. Siepmann, J. Phys. Chem. B 102 (1998) 2569–2577.
[62] J.M. Smith, H.C. Van Ness, M.M. Abbott, Introduction to Chemical Engineering Thermodynamics, 7th ed., McGraw-Hill, New York, 2005.
[63] J.J. Potoff, A.Z. Panagiotopoulos, J. Chem. Phys. 109 (1998) 10914–10920.
[64] H.A. Lorentz, Ann. Phys. 12 (1881) 127–136.
[65] D.C. Berthelot, Compt. Rend. 126 (1898) 1703–1706.
[66] P.P. Ewald, Ann. Phys. 64 (1921) 253–287.

[67] P. Atkins, J. de Paula, Atkins' Physical Chemistry, 7th ed., Oxford University Press, New York, 2002.

[68] D.-Y. Peng, D.B. Robinson, Ind. Eng. Chem. Fundam. 15 (1976) 59–64.

[69] I. Langmuir, J. Am. Chem. Soc. 40 (1918) 1361–1368.

[70] T. Uchida, T. Hirano, T. Ebinuma, H. Narita, K. Gohara, S. Mae, R. Matsumoto, AIChE J. 45 (1999) 2641–2645.

[71] M.-K. Hsieh, W.-Y. Ting, Y.-P. Chen, P.-C. Chen, S.-T. Lin, L.-J. Chen, Fluid Phase Equilib. 325 (2012) 80–89.

[72] W.M. Deaton, E.M. Frost Jr., Gas Hydrates and Their Relation to the Operation of Natural Gas Pipelines, U.S. Bureau of Mines Monograph 8, 1946.

[73] D.R. Marshall, S. Saito, R. Kobayashi, AIChE J. 10 (1964) 202–205.

[74] M.M. Conde, C. Vega, J. Chem. Phys. 133 (2010) 064507.

[75] B. Guillot, Y. Guissani, J. Chem. Phys. 99 (1993) 8075–8095.

[76] D. Paschek, J. Chem. Phys. 120 (2004) 6674–6690.[77] W.L. Jorgensen, J.D. Madura, Mol. Phys. 56 (1985) 1381–1392.

[77] H.W. Horn, W.C. Swope, J.W. Pitera, J.D. Madura, T.J. Dick, G.L. Hura, T. Head-Gordon, J. Chem. Phys. 120 (2004) 9665–9678.

[78] H. Docherty, A. Galindo, C. Vega, E. Sanz, J. Chem. Phys. 125 (2006) 074510.

[79] E.D. Sloan, F. Fleyfel, Fluid Phase Equilib. 76 (1992) 123–140.